Arnaud Caillet
ESI GmbH

Antoine Guellec
Audi AG

Denis Blanchet
ESI GmbH

Thomas Roy
EDAG GmbH & Co.KGaA

Abstract

Since the last decade, the automotive industry has expressed the need to better understand how the different trim parts interact together in a complete car up to 400 Hz for structureborne excitations. Classical FE methods in which the acoustic trim is represented as non-structural masses (NSM) and high damping or surface absorbers on the acoustic cavity can only be used at lower frequencies and do not provide insights into the interactions of the acoustic trims with the structure and the acoustic volume. It was demonstrated in several papers that modelling the acoustic components using the poroelastic finite element method (PEM) can yield accurate vibro-acoustic response such as transmission loss of a car component [1,2,3]. The increase of performance of today's computers and the further optimization of commercial simulation codes allow computations on full vehicle level [4,5,6] with adequate accuracy and computation times, which is essential for a car OEM.

This paper presents a study of a fully trimmed vehicle excited by structureborne excitations with almost all acoustic trims such as seats, dash insulator, instrument panel, headliner… which are modelled as poroelastic finite element (PEM) parts. Simulation results are compared with extensive measurement results. The interactions between structure, acoustic trims and acoustic volume are illustrated and finally the analysis of several design changes such as trim material properties or geometry modifications is demonstrated.

Classical FEM Modeling Method for Trims

The classical way to model a fully trimmed vehicle for vibro-acoustic studies is illustrated in Figure 1. Most of the interior parts of the passenger cabin are built as concentrated masses except for the front seats, the instrument panel and the HVAC which are modeled explicitly. Trim components like carpets and insulation are represented as nonstructural masses. Cover parts, such as the door panels are represented as concentrated masses hanging on panels attachment points. Speakers, servomotors or control units are rigid bodies, whose masses are defined by modifying their density. Damping pads are also included in the FE model, built with a 3 layer solid mesh (Figure 2).

The acoustic energy dissipation can be represented by two methods in the classical full vehicle models. The simplest way is to define a lossfactor in the material card of the fluid, but there are limitations. Firstly, it is difficult to get the right value which describes the acoustic behavior of all the interior parts. State of the art values are close to 20% damping. Secondly, it is not possible to define frequency dependent damping. Another way is to apply frequency-dependent absorption to the surface of the acoustic cavity. This leads to more accurate results but requires measured values as input and much longer computation times.

Figure 3 shows the distribution of the frequency-dependent acoustic absorber elements. The acoustic properties for each trim panel are taken from former measurements in a similar car

project. Inside the fluid only spaces for the seats are left empty. The parcel shelf is not considered. The interior cavity is modeled as a single volume.

Other harsh limitations of this method are that the thickness variation of the acoustic trims, the interaction between trim panels and structure and the contribution of the trim panels, radiating into the interior cavity, are not represented.
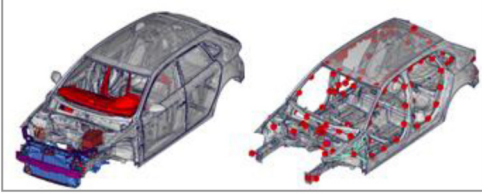

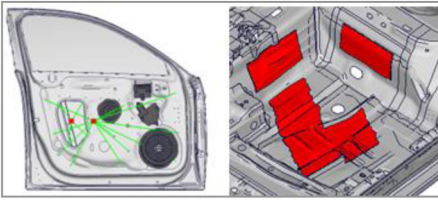Figure 1. Full Vehicle structural FEM model (left) and local masses in body model (right)

Figure 2. Local mass representing door panel (left) and damping pads on car floor as solid elements (right)
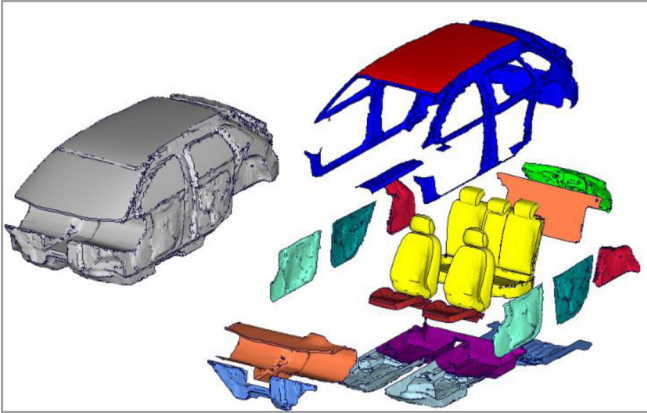

Figure 3. Interior acoustic cavity (left), Surface Absorption (one color, one value) (right)

Theoretical Background

Porous Material Modelling

As described in [7,8,9], propagation of elastic and acoustic harmonic waves, with an $e^{-i\omega t}$ time dependency, in porous elastic media is governed by the following system of modified Biot's equations:

$$\widetilde{\rho}_s\, \omega^2 U + \mathrm{div}\left(\sigma^s_{kl}(U) - \widetilde{\alpha}\phi\, p \delta_{kl}\right) + \dots$$
$$\dots \widetilde{\beta}\,\mathrm{grad}(\phi p) = 0$$

(1)

$$\mathrm{div}(\frac{1}{\omega^2 \widetilde{\rho}_f}\,\mathrm{grad}(\phi p) - \widetilde{\beta} U) + \frac{\phi p}{R} + \dots$$
$$\dots \widetilde{\alpha}\,\mathrm{div}(U) = 0$$

(2)

Where:

The vector U represents the skeleton displacement, σ^s_{kl} the components of the stress tensor in the skeleton and p the acoustic pressure. ω is the angular frequency, Φ is the porosity and $\widetilde{\rho}_s$, $\widetilde{\rho}_f$ are respectively the skeleton and fluid equivalent mass densities, which are related to the real mass densities ρ_s ρ_f of the structure and fluid by:

$$\widetilde{\rho}_s = (1 - \phi)\rho_s + \phi \rho_f\left(1 - \frac{\rho_f}{\rho_e}\right)$$

(3)

$$\widetilde{\rho}_f = \phi \rho_e$$

(4)

Where ρ_e is the effective mass of the interstitial fluid given in [9]. Equation 5 represents the inertial coupling factor and equation 6 represents the stiffness coupling factor.

$$\widetilde{\beta} = \frac{\rho_f}{\rho_e} \qquad \phi\widetilde{\alpha} = 1 - \frac{K_b}{K_s}$$

(5,6)

The coefficient R represents the bulk modulus of the porous elastic media.

$$R = \frac{K_s \phi^2}{1 - \phi - K_b / K_s + \phi K_s / K_e}$$

(7)

The coefficients K_b, K_s represent respectively the bulk modulus of the skeleton with vacuum inside and of the material of the skeleton, and finally K_e represents the effective bulk modulus of the interstitial fluid as given in reference [9].

Biot Parameters Identification

Ten years ago, only few engineers had the opportunity to work with Biot parameters. Just a handful of laboratories were able to provide these values based on extensive sophisticated measurements. Fortunately, today's situation has drastically changed. Biot parameters can be identified using an indirect method. Based on a simple impedance tube measurement (Figure 4) and the measurement of acoustic porosity and air flow resistivity which can now be determined experimentally with reasonable accuracy, the acoustic Biot parameters (Φ open porosity, σ static airflow resistivity, α∞ geometrical tortuosity, λ viscous characteristic length, λ' thermal characteristic length) can then be calculated using different optimization algorithms [10,11,12]. These identified Biot

parameters are the intrinsic properties of the poro-elastic properties because only one set of parameter values is possible in the solution. To fully characterize foam type material extra properties such as Young's modulus and damping of the foam structure is needed. These are easily obtained from a quasi-static mechanical test. Figure 5 shows the sensitivity of the different Biot parameters over the frequency range.
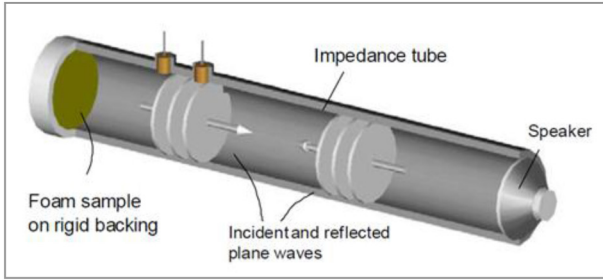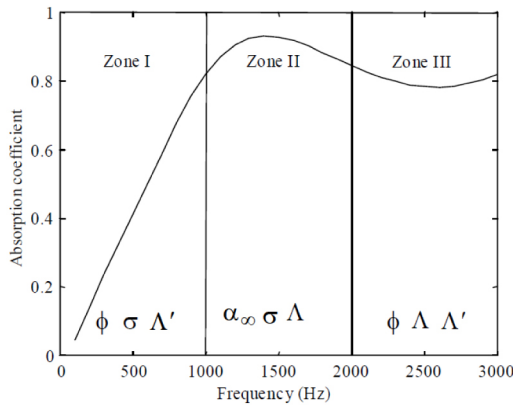

Figure 4. Impedance tube

Figure 5. Frequency zones of a typical Biot parameter

Full Vehicle Modeling

As described in [13], the trim of a full vehicle analysis can be added to the classical structure/fluid coupled linear system as a trim impedance matrix $\widetilde{Y}$.

The dynamic equation of the trimmed vehicle can be written in the following form:

$$\left[\begin{pmatrix} Z_s & C_{sc} \\ C_{sc}^t & A_c \end{pmatrix} + \begin{pmatrix} \widetilde{Y}_{ss} & \widetilde{Y}_{sc} \\ \widetilde{Y}_{sc}^t & \widetilde{Y}_{cc} \end{pmatrix} \right] \begin{bmatrix} U \\ P \end{bmatrix} = \begin{bmatrix} F \\ Q \end{bmatrix}$$

(8)

Where Z_s is the mechanical impedance of the master-structure (car body in white), A_c is the acoustic admittance of the internal cavity. C_{sc} is the surface coupling operator between the untrimmed master-structure surfaces directly in contact with the internal acoustic cavity.

U is the displacement field vector of the master-structure, P the pressure field of the internal cavity; F the external force field applied to the master-structure, and Q represents internal acoustic sources. The matrix $\widetilde{Y} = R'YR$ is the transferred impedance matrix of the porous component where R is the transfer operator relating the degrees of freedom of the porous component to the degrees of freedom of the master structure and of the internal cavity.

The linear system of equations (8) is solved using structural and acoustic normal modes. This has the great advantage of keeping the trimmed linear system to be solved at the same size as the initial BIW linear system.
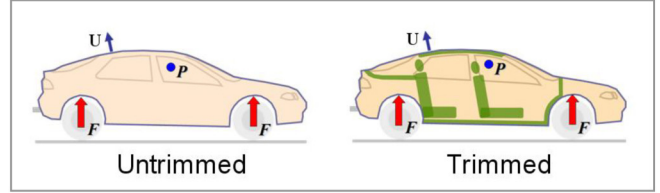

Figure 6. Untrimmed and trimmed configuration

Academic Case

In order to show the principles of the PEM method and its benefits, a simple test case (description on Figure 7) was first investigated. Measurements, simulations with classical NSM + high acoustic damping trim representation and simulations with trim as PEM with Biot parameters are compared.

The simulation and test data presented here for the Biot case have been done independently without any tuning (blind simulation results).

The presence of the trim has a dramatic effect on the panel velocity, damping all the peaks except for the first few ones (see Figure 8 and [13]). The Biot formulation predicts this phenomenon very well. The NSM approach alone cannot model the correct behavior of the plate. A trial and error approach is used to find suitable structural damping values (20%) to apply on the base panel in order to match the measured panel velocity. In the cavity, a 20% damping value was applied.
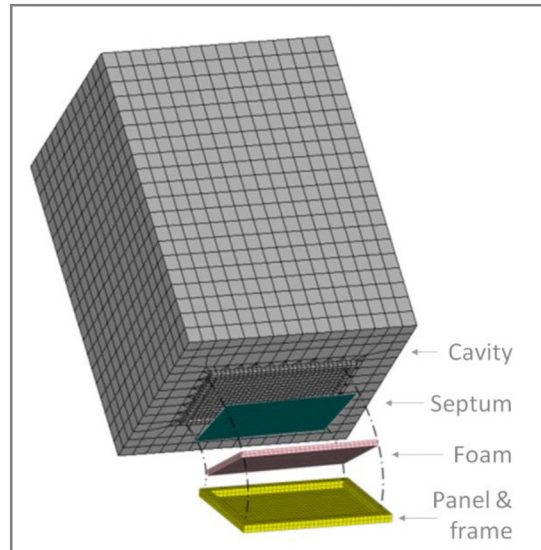

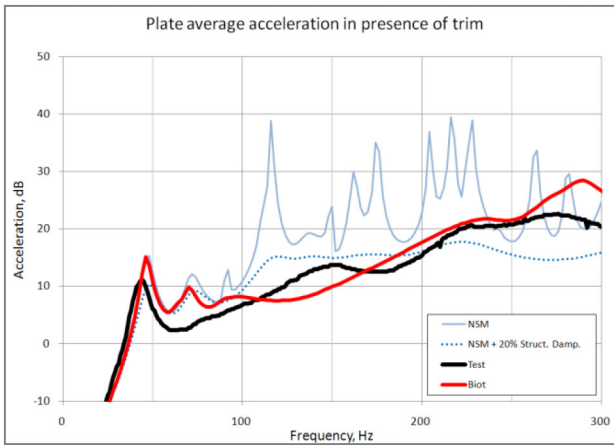Figure 7. General arrangement of RTC3 case.

Figure 8. Plate average acceleration

The same phenomena can be observed with the average pressure in the cavity (see Figure 9). As a conclusion, NSM by itself is insufficient to represent the physics of the problem.
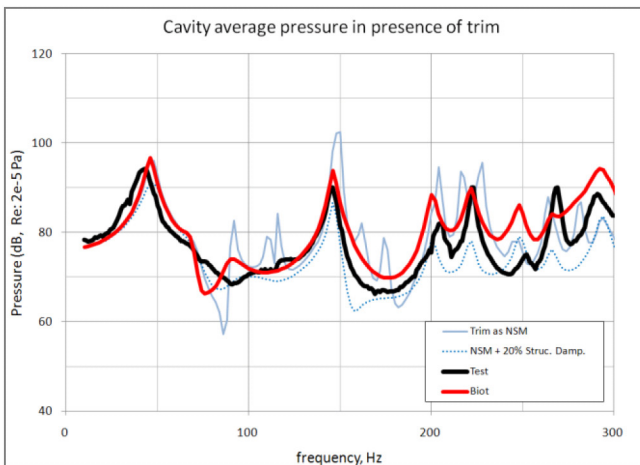

Figure 9. Cavity Average Pressure

Full Vehicle Model Creation Process

Structural Mesh

The structural mesh of a typical NVH trimmed body model can be used as a basis model to be enhanced into a full vehicle model with PEM. The modal basis is computed on the complete vehicle trimmed body model and exported on a reduced set of nodes (see Figure 10) to optimize the computation time and the space required to store the data. Only the nodes and elements which are candidate to be coupled to the acoustic and trim domains are included in this reduced model. Excitation and results recovery nodes should also be included. This reduces the amount of nodes for which the modal basis is exported from 1524982 to 415718 nodes. The modal basis is computed up to 1,3 times the maximum frequency of coupled response computation. About 2300 modes are computed up to 520Hz to evaluate a coupled response up to 400Hz. Modal damping is computed during the modal extraction. This modal damping matrix is used to model the damping coming from structural parts and damping pads

included in the structure. Damping pads are modeled as solid elements as explained in chapter "Classical modeling method for trims".

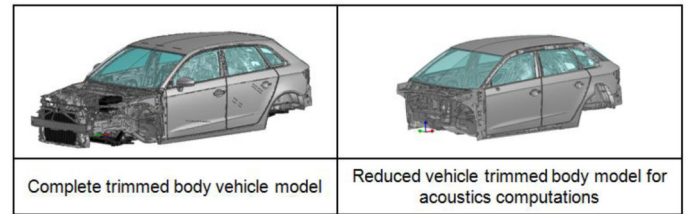| Complete trimmed body vehicle model | Reduced vehicle trimmed body model for acoustics computations |

Figure 10. Structural mesh

Acoustic Mesh

The acoustic cavity mesh (Figure 11) is morphed with the trim shape and the structure to ensure an appropriate coupling between the structure, the trim and the fluid. The size of the interior elements is chosen according to the rule of 6 elements per wavelength. For the surface of the cavity, to ensure a good coupling between the trim, the structure and the acoustic domains, the mesh size should be at least twice as big as the element size of the trim/structure. The cavity is made of 540226 tetra linear elements and 111494 nodes.
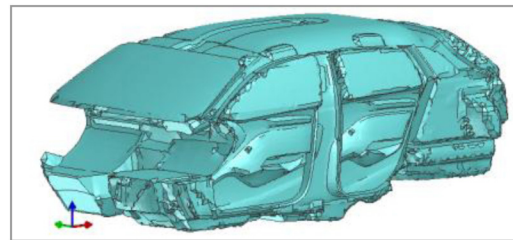

Figure 11. Acoustic mesh

Trim Mesh

Trim meshes are generated from CAD and trim layups descriptions provided in constructions drawing (see figure 13). In the studied model, quadratic solid elements with a size of 20 to 30mm in the plane direction of the part are used. For the normal direction of the mesh, the actual thicknesses of the trim are used with a maximum thickness of 10mm. The discretization of the trim parts with such elements will ensure a reasonable good representation of the physics up to 400Hz. A. Duval describes this process in [1,14].

In the example presented here, the following parts are converted from non structural masses or point masses in the old model to physically represented trims: dash insulator, instrument panel, headliner, seats front and rear, floor carpet, door panels, package tray, trunk floor, trunk compartment trims, A,B,C,D pillars trims. On Figure 13, an overview of all the trim meshes is shown. The trim parts in the model contain 994931 nodes, 600739 elements.

For each trim an impedance matrix is computed. The size of this matrix is proportional to the number of structural and acoustic modes. These impedances will be used ultimately to represent each trim in the model during the computation of the coupled response. To compute the trim impedances, a

frequency interpolation step of 20Hz is chosen. Impedance curves are usually monotonous and do not need a fine resolution (e.g. 1Hz). Absorption, insertion loss and damping effects of each trim are represented in the impedance matrices.

Some trims should be grouped together to form a subassembly trim. This is the case for the inner dash insulator and instrument panel, the rear wheelhouses and trunk compartment trim. In the following sections, the article will focus on the trunk trim because this part is representative for complex trims located in the car. The trunk trim construction is detailed in Figure 14 for the mesh and on Figure 15 for the integration in the real car. This trim contains 3 parts:

- The plastic trunk panel is displayed on the left side of Figure 14. This part is made of an elastic solid material representing the plastic trunk trim. At some locations, the plastic is covered by a thin layer of fiber as it is in the car. Biot parameters are used to model this layer. On Figure 16 a comparison between the real part and the mesh of the trunk plastic trim is shown. Some of the structural connections between the trunk plastic trim part and the structure are highlighted on Figure 16. These connections are included as solid elements in the mesh to allow the structureborne energy to flow from the structure to the trim and let the trim panels radiate into the trunk cavity as in reality. Specific boundary conditions are applied to these elements. This will be described in the section entitled "Coupling".
- The wheelhouse absorbers are displayed on right side of Figure 14. This trim is made of several porous material layers. For this part, Biot properties have been identified for each layer and assigned to the mesh. The wheelhouse absorbers are directly laying on the wheelhouse structure as illustrated on left side of Figure 15.
- The Airgap between wheelhouse absorbers and plastic panels is represented in the middle of Figure 14. This part has a high thickness variability to model properly the empty space filled by air. The interface nodes between the air gap and the others trims of the trunk region (wheelhouses absorbers and trunk trim) are merged to create a single mesh. This allows the energy to flow freely from one trim part to another. Where no trim is laying on the structure, the air gap is morphed to the shape of the structure to ensure an optimal coupling.

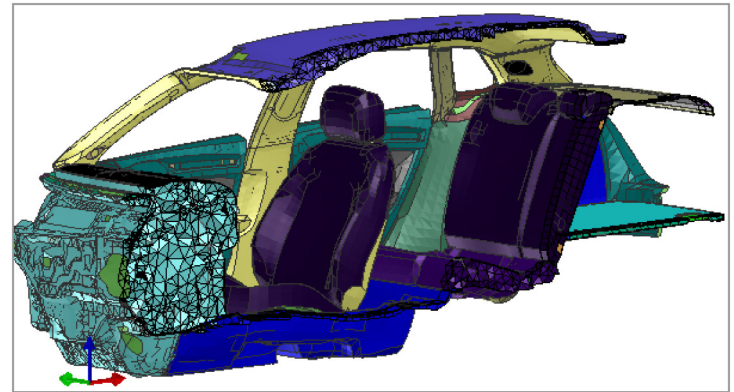Figure 12. Trim meshing process, example of a rear wheelhouse absorber
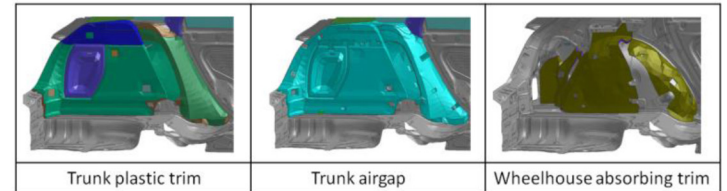

Figure 13. Trim meshes

Figure 14. Detail of trunk trim individual layers meshes
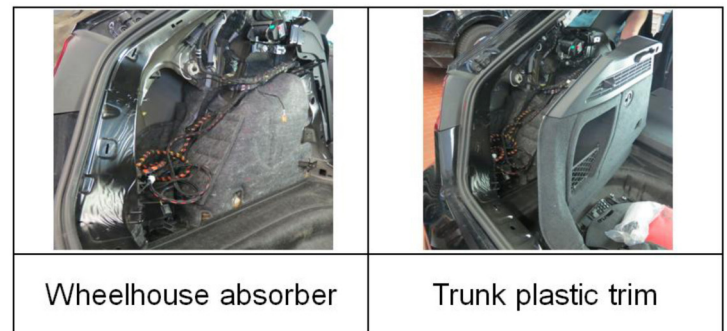
Figure 15. Trunk trims in the real car

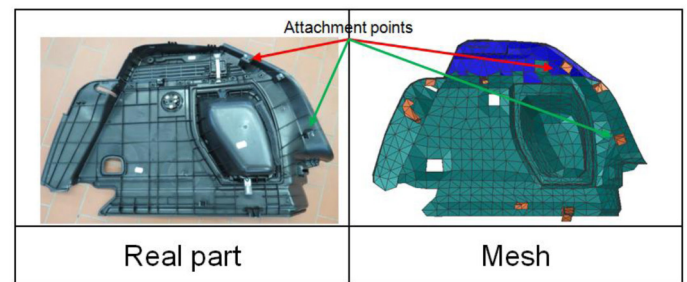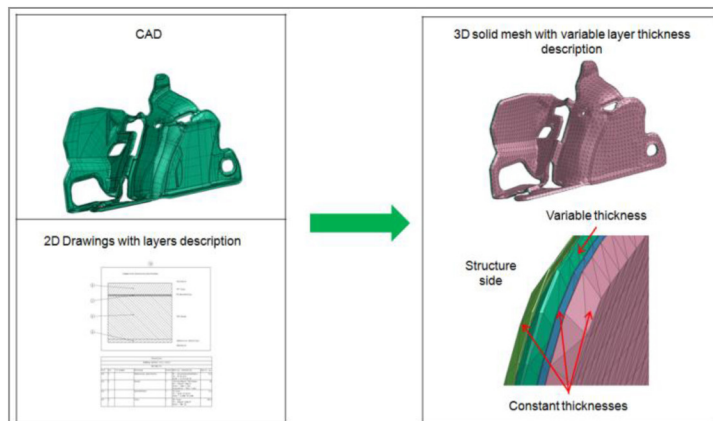Figure 16. Trunk plastic trim mesh comparison to real part

Biot Parameters Identification

To get an accurate representation of the physics for each trim part, 15 samples of different trims were sent to a laboratory to identify their Biot parameters. For some trim parts, it is necessary to perform several material characterizations since the Biot parameters change with the material compression rate. For each 5mm variation of the thickness distribution, Biot parameters were identified. See the "Biot parameters identification" chapter for more details about this.

Coupling

Boundary conditions are defined at the surface of each trim. It is important to define the boundary condition according to the real conditions in the car to model the physics correctly. From the definition of the boundary conditions and the coupling distance definition, ESI's VPS solver will run a dedicated algorithm to evaluate coupling between the different domains of the model. This coupling can be visualized within ESI's Visual-VTM FEM preprocessor. Different coupling definitions are possible for structure and acoustic parts as detailed below:

Most of the trim parts (floor carpet, inner dash insulator…) are laying on the structure. In that case, trim meshes are coupled to the structure with a **sliding boundary condition** [15,16]. All plastic trims are attached to the structure at locations which are representative of the reality. For these locations, a different boundary condition is used. The trim parts are coupled to the fluid with a **"perforated" boundary condition** when the cells of the foam are open at the surface of the trim. If the surface of the trim is covered by an impervious film or leather, the **"not perforated" boundary condition** is used. For all plastic parts coupled to the fluid, the "not perforated" boundary condition is used.

This paragraph will now put more emphasis on the trunk trims. On figure 17 the fixation points of the trunk trim to the structure are shown. Usually the boundary condition type chosen for these points is "fixed". The fixed boundary condition means that the coupled nodes of the structure and of the trim have the same displacements for all degrees of freedom. Figure 17 is showing one of these connection points between the trim and the structure. The trim mesh is very close to the structure and ensures an appropriate coupling and transfer of energy between the structure and the trim. On Figure 18 the influence of modifying the boundary conditions can be observed. On the driving point inertance, the influence is very limited even if the excitation is very close to the studied trim (see Figure 19). As the trim is much lighter than the total mass of the car, no big influence is seen when the boundary conditions change. However, for a microphone located in the trunk, differences can be observed. As boundary conditions are different, the trim will move differently and radiate noise differently to the acoustic cavity. The other elements of this trim which are coupled to the structure are set with a sliding boundary condition. Coupling definition on the fluid side is illustrated on Figure 18. Where the plastic panel is covered by the thin fiber layer the perforated boundary condition is used to take account of the absorption generated by the fiber. On the rest of the interior side of the trim the unperforated boundary condition type is used.
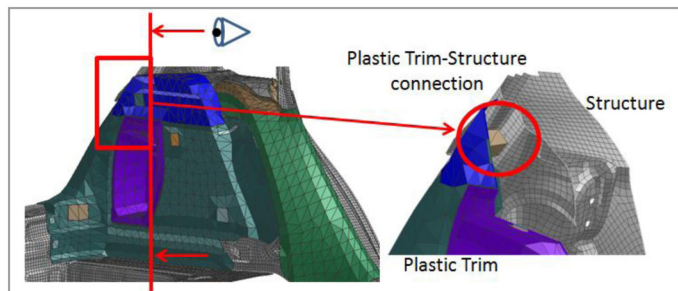

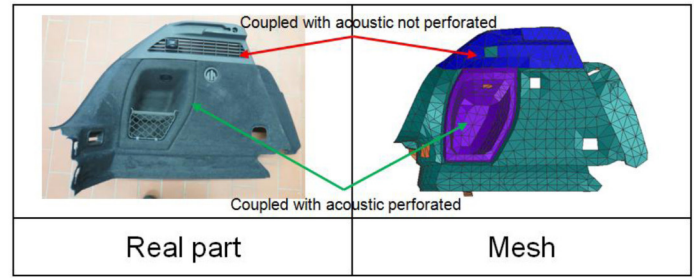Figure 17. Detail of trunk trim: connection to structure

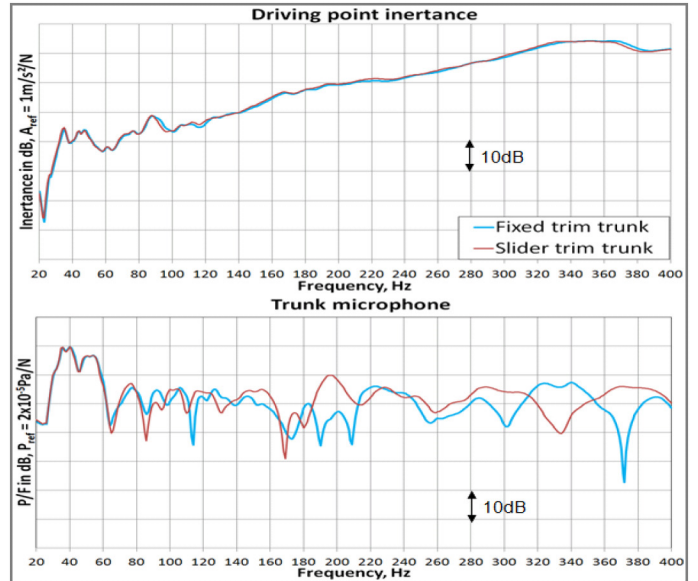Figure 18. Trunk trim acoustic coupling definition

Figure 19. Trunk trim structural boundary conditions changes influence

Sub-Assembly Models Validation

For some sub-assembly trims, individual investigations were done to validate the meshes. A transmission loss analysis was done for the inner dash insulator including the instrument panel. The front car structure and trim were measured in a transmission loss suite in order to investigate the airborne performances of the sub-assembly. A simulation model was built to replicate this test. The model is illustrated on Figure 20. The correlation between the measurement and the simulation are presented on Figure 21. More details about this component airborne analysis are presented by J.-F. Rondeau in [17].
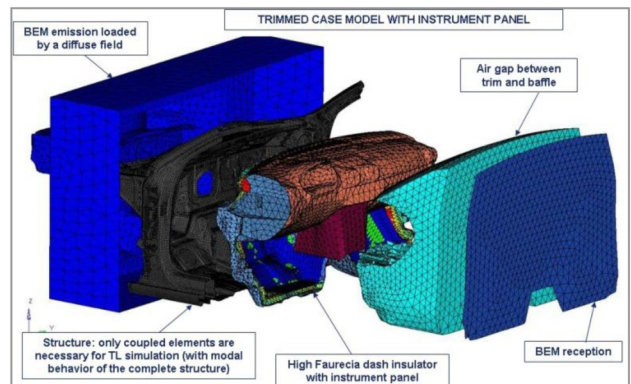

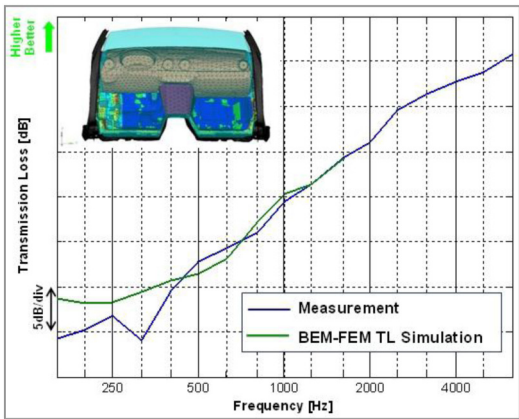Figure 20. BEM/FEM TL model with instrument panel

Figure 21. BEM/FEM TL simulation vs measurement correlation with Instrument panel

BIW Validation

Measurement Setup

To validate the structural model, measurements were done on a BIW structure of an Audi A3 5 doors. Excitations at several locations were applied and vibrations were measured at 125 points spread over the structure. These 125 accelerometers were grouped into several "radiating" panels (like floor, rear seat panel, firewall, windshield…) with at least 5 accelerometers for each of them. The average measured velocity over these panels is compared to the results obtained with the FE model. Figure 22 illustrates the excitation point and one of the analyzed panels. On Figure 23 pictures of the measurement points on rear wheelhouse left are presented.
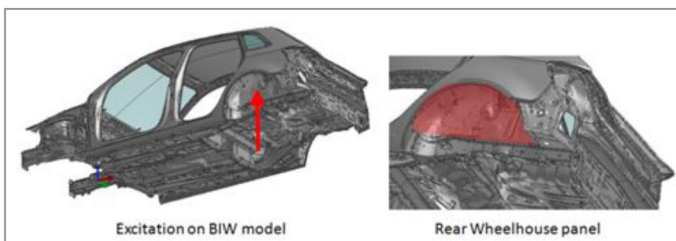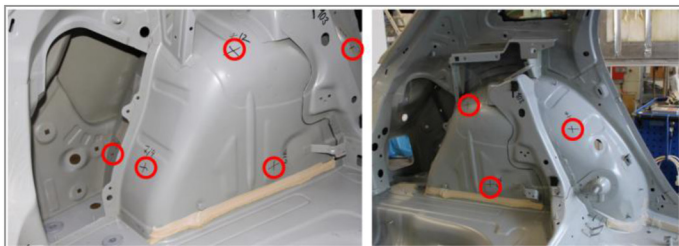

Figure 22. Excitation and studied panel for BIW

Figure 23. Excitation and studied panel for BIW

BIW FEM Model Validation

On Figure 24 the simulation and measurement results for an excitation are compared at rear suspension mount for frequency range [20;1000]Hz. On driving point inertance, the trend and the level are well represented by the FEM simulation for the complete frequency domain except between 200 and 450Hz. Between these two frequencies an offset can be observed. The average inertance on rear wheelhouse left

panel has a similar behavior. Until 300Hz, level and trend are well described by the FE model. Between 300 and 650Hz the trend of the measurement is represented by the FEM model. Then the two curves start to have a different behavior. Better correlations are observed for other panels like floor, roof and firewall. As these panels are the ones which radiate the most into the car, it can be assumed that the BIW structure is well represented by the FEM model. The BIW model will be used as a basis to build the fully trimmed model.
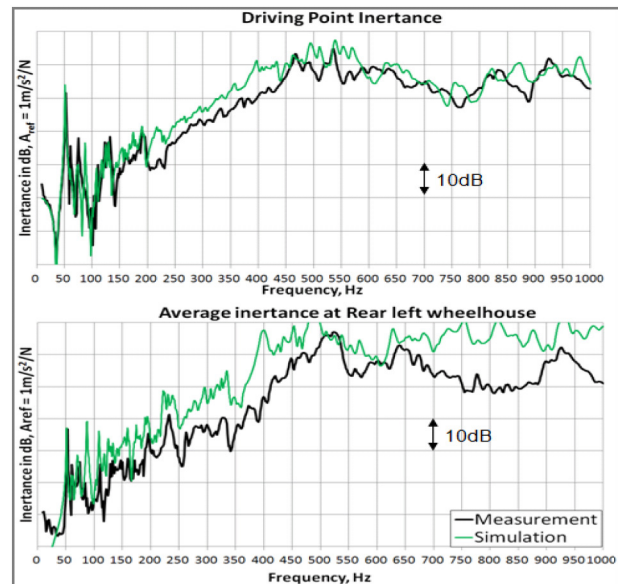

Figure 24. BIW Driving point inertance (left) and rear wheel house left average inertance

Trimmed Body Model Structural Improvements

In the measurement, a massive aluminum part is used at the excitation location to allow the test engineer to properly excite the car at the rear suspension mount. On Figure 25 the measurement setup is shown and how it is replicated in the FEM model by using rigid elements and a point mass. Different masses and rigid element lengths (d) were tested in the FEM model to find the best combination for the 3 excitation directions. The results of this study are displayed on Figure 25. A big influence of the distance and the mass can be seen on the diagrams for each direction. An improvement is seen from base configuration (red, no mass, d = 0mm) to the best one in light blue (M=900g, d=30mm). The analysis was made with an Audi A3 3 doors. This best configuration for this car was used in the FEM model for the further investigations on the Audi A3 5 doors.
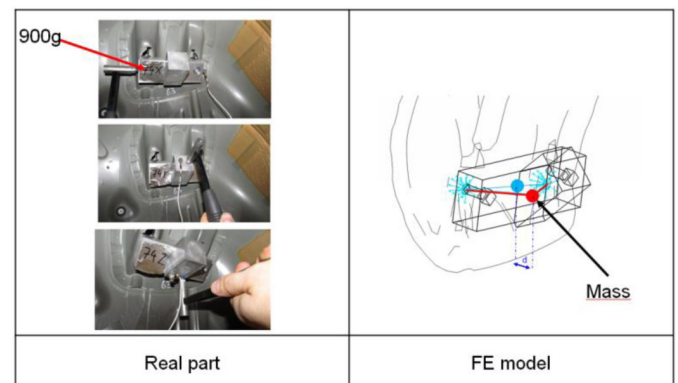

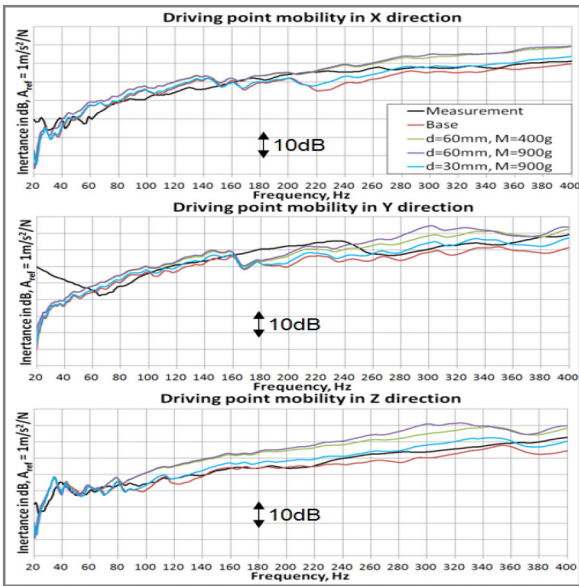Figure 25. Excitation at rear left suspension mount modelling

Figure 26. Driving point inertance modeling investigation at rear left suspension mount

Trimmed Body Model Investigations

Measurements

A 5 doors Audi A3 was measured. The vehicle was setup as a trimmed body. The car was excited at several locations. In the complete article the results are displayed for an excitation on the rear left suspension mount (Figure 27).
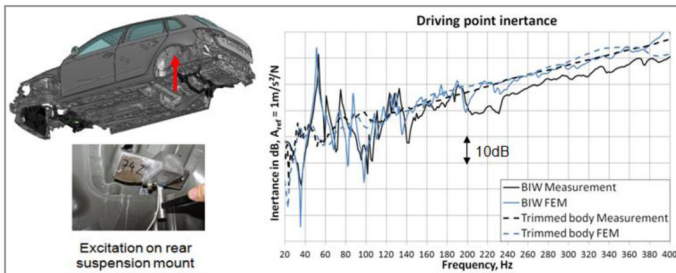

Figure 27. Excitation and measurement points on the floor

Figure 28. Microphones location for trimmed body measurements

On the right side of Figure 27 driving point inertances are displayed for measurement (black) and FEM simulations (blue) in the case of the BIW (continuous lines) and trimmed body (dash lines). A damping effect can be observed by comparing BIW and trimmed body. This is due to the parts

added into the car. All curves are very close except the BIW measured curve above 200Hz. This was studied in the BIW investigation paragraph.

Computation Parameters

Structural and acoustic modes are computed with MSC Nastran software. The modal basis is computed up to 1,3x maximum frequency of the coupled response. A specific DMAP is used to recover the modal damping matrix from the Nastran computation. Impedance matrices and coupled response are computed with ESI's VPS software [16]. Computation impedance matrices and coupled response on a 16CPU modern computer is an overnight task.

Validation against Measurement and Comparison to Classical FEM Methods

Measurement and PEM simulation results are now compared to results obtained with the classical method using Non-Structural Masses and Surface Impedances to model the car interior trim parts. The surface impedances were measured directly on the car. The results are shown on Figure 29.

The driving point inertance curves computed with both methods are very close to the measurement until 300Hz. After this frequency both simulations are slightly diverging from the measurement. This means that the modal basis may have to be computed up to higher frequencies.
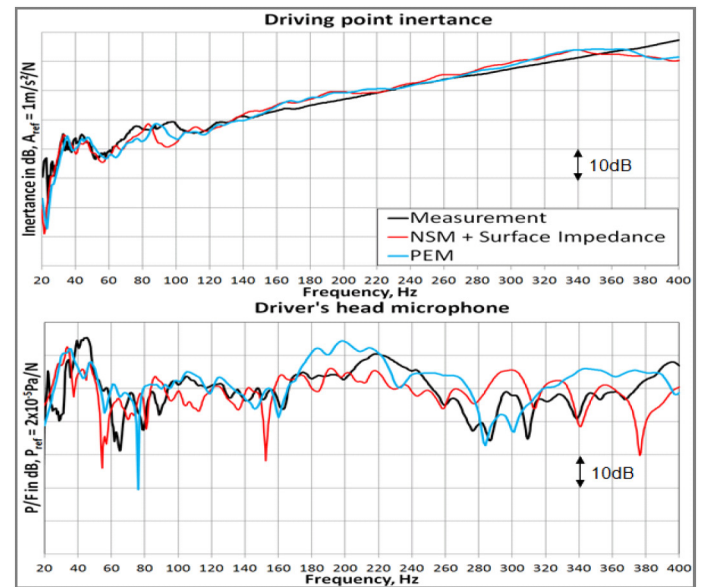

Figure 29. Measurement vs PEM vs NSM + Surface impedance results

Pressure is presented for driver's head location. Both NSM/ surface impedances and PEM simulations show globally reasonable results. The PEM simulation gives a curve which is slightly more representative of the behavior in measurements. Between 80 and 180Hz, PEM and measurement curves are quite close. Then the difference between simulation and measurement gets worse, in a range around 10dB. The trend of the measurement seems to be better predicted by the PEM

computation even if shifts in frequency are observed. The NSM + surface absorption curve is oscillating around an average level of the measurement curve.

Model Investigation

The aim of this part is to analyze the influence of a specific trim on sound pressure level at the driver's ear. Two variants of the model were run one including the trunk trim, one without it. In the case when the trunk trim is excluded from the model a new cavity is created. The structure will radiate directly to the interior of the model (Figure 30, lower picture). Package tray and trunk floor were also excluded from the model without trunk trim. This analysis will show how much influence the trunk trim has on the interior sound pressure level. Further measurements will be done later to validate the sensitivity of the model to this modification (not shown here).

Figure 31 shows the influence of including the trunk trim in the model. A slight influence can be seen on the driving point inertance. The trim is loading the model at the excitation point and a small effect can be observed particularly at 80Hz. On pressure at driver's head it can be observed that the sound pressure level is globally higher of 3dB without the trunk trim, which can be interpreted as the acoustic impact of the trunk trim. In the model without the trim, the structure radiates directly into the inner cavity. Absorption is also lower since the wheelhouse absorbers are not included in this variant.

A rear-axle rolling noise real life excitation has also been investigated for these 2 configurations. The excitation points are shown on Figure 32. The results can be observed on Figure 31. A positive effect of the trunk trim is seen. It is particularly interesting to see it in the frequency range [200; 240] Hz which is characteristic for torus noise. Including trunk trims (plastic trims and wheelhouse absorbers) has a great influence on sound pressure levels at all microphones from 180Hz to 400Hz (upper limit of the computation), which fits quite well with the experience from the test.

Figure 30. Audi A3 FEM-PEM model with the trunk trim (upper picture), without the trunk trim (lower picture)
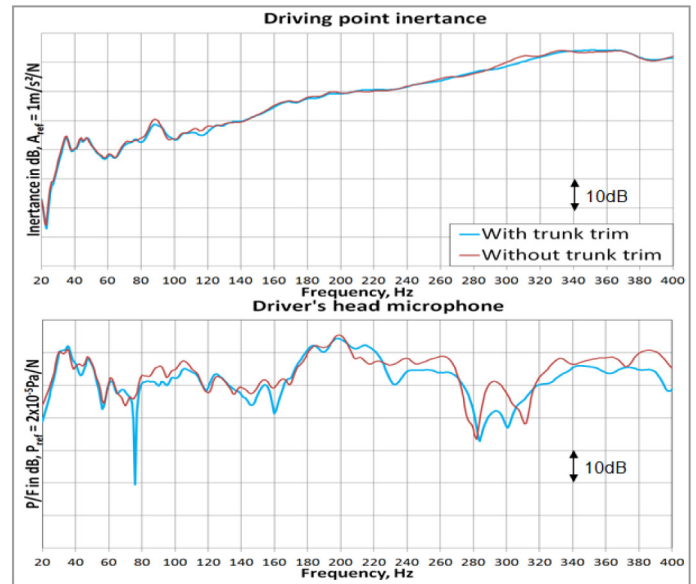

Figure 31. Influence of the trunk trim in the full vehicle model
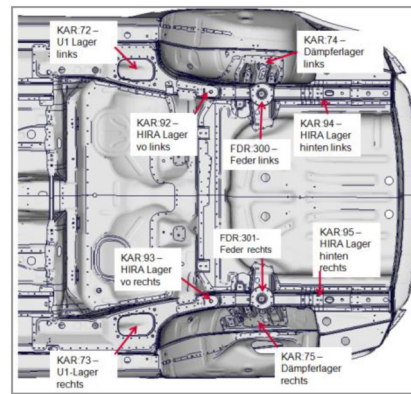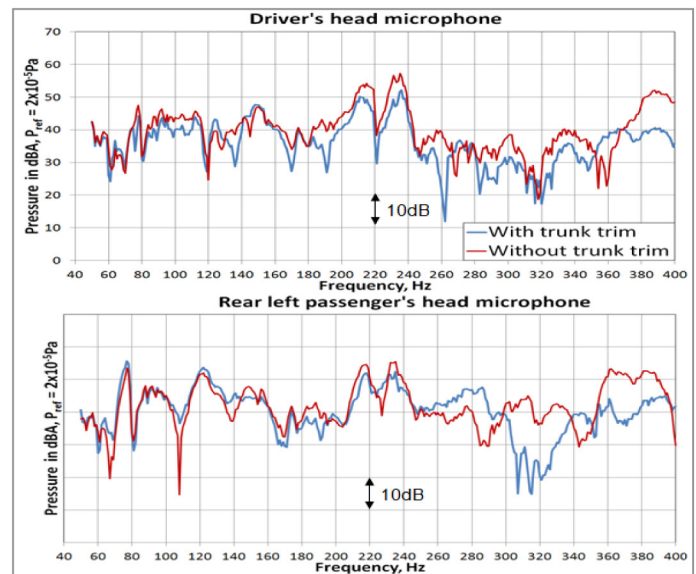

Figure 32. Rear axle rolling noise excitation locations
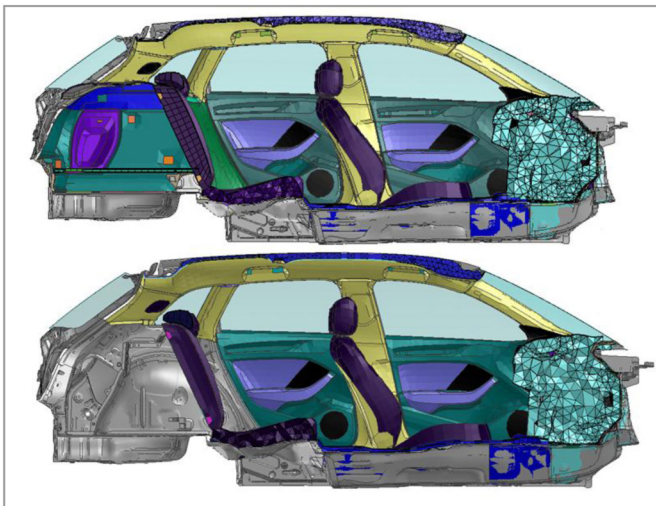

Figure 33. Rear axle rolling noise at driver's head

Perspectives

Even if a detailed correlation work has been done and many data have been collected and analyzed, systematic discrepancies between test and simulation could not be improved. This is due to the high complexity of the model that makes it very difficult to find out which parameter should be changed in order to improve the correlation. Another important aspect, the correlation of sensitivities or the capability of the model to predict the impact of modifications in the trim or in the structure was not part of the previous work.

For those reasons a more extensive measurement campaign will be run to validate individually each of the trim meshes and check the sensitivity of each trim to diverse parameters. Therefore another correlation method has to be defined. One method would be to validate separately in a TL-suite each subsystem in a similar way to the correlation project of the dash and IP model (p.7). Another more accurate method would be to compare the impact of separate trim components (like the trim model of the trunk) in the fully trimmed body in test and simulation and try to validate it. A mask method will be used to investigate the contribution of single trims to the pressure at a microphone. Airborne and structureborne excitations will be investigated. Analysis tools like intensity maps, panel/modal contribution will also be part of the correlation.

The absolute correlation of the acoustic response is less important than the capability of the model to correctly predict the impact of structural and trim modifications and provide realistic sensitivities. A full vehicle PEM that would be validated for that would open new perspectives to understand acoustic phenomena in the low to mid frequencies and to find faster solutions to acoustic issues. It will also be a great tool in the development of always more performing, less expensive and lighter acoustic packages, ideally combining structure and trim interactions. Another interesting aspect is that it opens new perspectives in the development process with suppliers of acoustic components.

A great challenge will be the improvement of the modeling guidelines, another one will be the improvement of the computation times and stability; the last and maybe the bigger challenge will be the integration of this method in the CAE-process, which will require much more efforts and skills than in the past.

Conclusions

In this paper a method to create and validate fully trimmed FEM vehicle model with trims represented as PEM is presented. From CAD parts and 2D drawings, PEM trim meshes were generated and assembled within a FEM structural and acoustic model of a complete car. This detailed method takes account of the thickness variation within each trim and of the complex porous physical properties using the Biot parameters. The different parts can be validated by running component analysis and then assembled into the full vehicle model. Even if this process needs more modeling and computation efforts compared to the classical NSM + surface absorption method, it provides a higher accuracy for the SPL prediction and gives the possibility to deeper understand the complex behavior of each trim part in the car (radiation of plastic trims, absorption of acoustic trims, interactions trim to structure, development of mass spring systems…). These extra capabilities open many new perspectives in order to improve the efficiency of the ground acoustic development of a new vehicle, the acoustic development of separated acoustic component like a dash insulator, and also to understand complex mechanisms of acoustic phenomena in real life excitation and as a consequence to solve faster mid frequency acoustic issues.

Acknowledgements

References

1. DUVAL A. and al.: "Trim FEM simulation of a dash and floor insulator cut out modules with structureborne and airborne excitations", In Euronoise-Acoustics'08, Paris, France, 2008.

2. Omrani A. and al.: "Transmission loss modeling of trimmed vehicle components", ISMA-2006

3. Omrani A. and al.: "Theoretical foundation for the modeling of transmission loss for trimmed panels, JSAE, 2007

4. ANCIANT M. and al.: Full trimmed vehicle simulation by using Rayon-VTM., In JSAE, Japan, 2006.

5. Blanchet D. and al.: "Modeling the vibro-acoustic effect of trim on full vehicle and component level analysis", DAGA, 2009

6. Blanchet D. and al.: "Acoustic trim modeling: traditional spring/mass system vs Biot theory", EAA Euroregio Ljubjana, 2010

7. Atalla N. and al.: "A mixed pressure-displacement formulation for poroelastic materials" J. Acoust. Soc. Am., 104(3), 1444-1452, 1998

8. Atalla N. and al.: "Enhanced weak formulation for the mixed (u,p) poroelastic equations" J. Acoust. Soc. Am., 109(6), 3065-3068, 2001

9. Allard, J. F.: "Propagation of Sound in Porous Media, Modelling of sound absorption", Charpman & Hall, North Way Andover, Hampshire, SP105BE, England, 1993

10. Atalla Y., Panneton R: Inverse acoustic characterization of open cell porous media using impedance tube measurements, Canadian Acoustics, Vol 33 No.1, 2005

11. Panneton, R., Atalla, Y., Blanchet, D., and Bloor, M., "Validation of the Inverse Method of Acoustic Material Characterization," SAE Technical Paper 2003-01-1584, 2003, doi:10.4271/2003-01-1584.

12. FOAM-X User's guide

13. Hamdi M.A. and al.: "Analysis of vibro-acoustic performances of a fully trimmed vehicle using an innovative sub-system solving approach facilitating the cooperation between carmakers and sound package suppliers", Eurodyn 2005.

14. Duval A. and al.: "Structureborne and airborne Insertion Loss simulation of trimmed curved and flat panels using Rayon-VTMTL: implications for the 3D design of insulators", Automobile and Railroad Comfort, Le Mans, 2008

15. VTM User's Guide

16. VPS Solver reference guide

17. Rondeau, J., Dejaeger, L., Guellec, A., Caillet, A. et al., "Cockpit Module Analysis Using Poroelastic Finite Elements," SAE Technical Paper 2014-01-2078, 2014, doi:10.4271/2014-01-2078.

Contact Information

A. Caillet, ESI Group
arnaud.caillet@esi-group.com

A. Guellec, Audi
antoine.guellec@audi.de

T. Roy, EDAG
thomas.roy@edag.de

Definitions/Abbreviations

FRF - Frequency Response Function

BEM/FEM - Boundary/Finite Element Method

TL - Transmission Loss

PEM - Poro-Elastic finite element method

NSM - Non Structural Mass

BIW - Body in White

SPL - Sound pressure level

FMM/BEM - Fast multipole method Boundary element method

BC - Boundary condition